Signal Processing Tools for Non-Stationary Signals Detection

Thibaud Plazenet[1,2], Thierry Boileau[1], Cyrille Caironi[2], Babak Nahid-Mobarakeh[1]
[1]GREEN – Université de Lorraine, 2 avenue de Forêt-de-Haye, 54505 Vandœuvre-lès-Nancy, France
[2]LORELEC, 48 avenue Charles De Gaulle, 54425 Pulnoy, France

thibaud.plazenet@univ-lorraine.fr ; thierry.boileau@univ-lorraine.fr ; cyrille.caironi@caircy.org ; babak.nahid@univ-lorraine.fr

***Abstract*— In this paper we aim to compare the abilities and performances of signal processing tools to detect non-stationary signals coming from condition monitoring of electrical machines. From the vast amount of available tools, we focus on existing signal processing methods suitable for real applications for non-stationarities tracking and quantification over time which is particularly interesting in fault diagnosis. First, we assess the spectral kurtosis, a tool that gained much attention because of his capability to characterize transients masked by strong noises. In order to detect non-stationarities, other methods are evaluated such as the spectral subtraction through the short time Fourier transform or the Wiener filtering which can remove stationary components. The analytical framework of each tool is first presented. Non-stationary tests signals based on properties of vibration signals of bearings are proposed to compare effectiveness, advantages and drawbacks of each methods for non-stationarities detection. The purpose is to select a method that is best suited for each type of non-stationarity in order to improve the reliability of the detection.**

***Keywords*— non-stationary signal, spectral kurtosis, spectral subtraction, Wiener filtering, signal processing**

I. INTRODUCTION

Over the past decades, with the computing advances, complex signal processing tools have been commonly used in many applications. Simultaneously, signal processing methods including multiple variants and concatenation of tools have been extensively developed. Among this vast literature, we are focusing on tools that can be easily implemented on real life applications in order to enhance condition monitoring of systems and thus improve their reliability. In general signal encountered in real applications possess both stationary and non-stationary components often buried in strong background noises. In many applications, it is necessary to detect short duration and weak magnitude transients which can be challenging in some cases. Most mechanical and electrical faults in machinery have the characteristics of transient events in vibrations signals [1]–[3]. Moreover, speed and load variations create non-stationary conditions that compelled researchers to apply time-frequency methods in fault detection algorithms on both stator current and vibration signals [4]. We naturally look towards time-frequency methods as they reveal the time-dependent variations of signals. The spectral kurtosis (SK) is a spectral statistic tool that removes stationary frequencies and provides high response for transient frequencies. The spectral subtraction through the short time Fourier transform (STFT) [5] often used in audio noise cancellation purposes can also be used to enhance non-stationarities as it could suppress periodic spectral components. From the same point of view, the Wiener filter will be compared as it could serves the same purpose with less computing time [6], [7]. In the following sections, the signal processing tools will be theoretically presented as part of a condition monitoring system along with two types of synthesis non-stationary vibration signals based on properties of a bearing generalized roughness fault. Next, using these signals, the studied methods will be compared to find a trade-off between efficient non-stationary detection and computing time.

II. METHODOLOGIES

A. Spectral Kurtosis

In statistics, the kurtosis is a quantifying indicator of the tails of the probability distribution of a signal $x(n)$. This is the fourth standardized moment defined as [8]:

$$K(x) = \frac{\langle (x-\mu)^4 \rangle}{\sigma^4} - 3 \quad (1)$$

where μ and σ are the mean and standard deviation of $x(n)$ and $\langle \dots \rangle$ the expected value. With this definition, the kurtosis of a random signal is zero. According to [9], the spectral kurtosis can be defined as the fourth-order spectral moment:

$$SK_x(m) = \frac{\langle X(m)^4 \rangle}{\langle |X(m)^2| \rangle^2} - 2 \quad (2)$$

where $X(m)$ is the discrete Fourier transform (DFT) of $x(n)$. Then the SK of $x(n)$ can be interpreted as the kurtosis of $X(m)$ on each frequency m. To compute the SK, a minimum number of spectrum realizations are necessary, which means that the STFT has to be used. However, the window length could be difficult to find in order to maximize the SK, and hence maximize the transient detection. The kurtogram's method studied in [10] is a relatively quick method to compute the SK using either multirate filters or complex Morlet wavelets. It is used to select the best window length to

determine in which frequency band the kurtosis is at its maximum. In term of process condition monitoring, obtaining this frequency band is the first step to highlight the transient activity over time. The SK is computed between a reference state signal from the system and the next state signal by using the STFT with a fixed window length for a real time implementation. In [11] a SK based criterion is used to monitor defined bearing fault frequencies. Derived from this criterion a non-stationary criterion is proposed by only taking the positive values of the SK over all frequency m :

$$\chi_{SK} = \frac{\sum_m SK_{x_2}(m)^2}{\sum_m SK_{x_1}(m)^2} - 1 \; ; \; if \; SK(m) > 0 \qquad (3)$$

where x_1 and x_2 are the signals acquired from the monitored system respectively at time t_1 and t_2 with $t_2 > t_1$. To improve the signal-to-noise ratio (SNR), each SK is squared, minimizing values between zero and one. With the proposed definition, the criterion χ_{SK} is set at zero at the start of the monitoring.

B. *Spectral Subtraction*

The principle of the next methods is to enhanced non-stationarities by removing the stationary parts of the signals being monitored over time. The STFT is a time localized Fourier transform of a signal $x_1(n)$ using a sliding window function $w(n)$. The result is two-dimensional, provides time variation of the frequency content and is defined as:

$$X_1(m,\omega) = \sum_{k=0}^{N-1} x_1(k) w(k-m) e^{-j\omega k} \qquad (4)$$

where N stands for the number of samples and m the time index. The spectral subtraction based STFT as defined in [12] is performed during the condition monitoring between two states of the system in which $x_1(n)$ is considered as the initial reference for the system:

$$R(m,\omega) = |X_2(m,\omega) - X_1(m,\omega)| e^{\varphi(m,\omega)} \qquad (5)$$

where $\varphi(m,\omega)$ is the phase of $X_1(m,\omega)$ and $R(m,\omega)$ is the spectral residue containing non-stationarities. The inverse STFT is then computed to retrieve the temporal residue $r(n)$ which is an image of the non-stationarities. The absolute rms value of $r(n)$ is computed to obtain a readable criterion characterizing the evolution of the system between the two states:

$$\chi_{SS} = \frac{1}{N} \sum_{i=0}^{N-1} |r(i)|^2 \qquad (6)$$

C. *Wiener filtering*

The spectral subtraction can also be performed using a model of the system assuming that the reference signal $x_1(n)$ is a wide sense stationary process. This can be achieved through a Wiener filter which is an optimal estimation of $x_1(n)$ in the mean-square sense. As previously studied in [13], the prediction error ξ can be formulated as:

$$\xi = \langle \left| x_1(n) - \sum_{k=0}^{p} w(k) x_1(n-k) \right|^2 \rangle \qquad (7)$$

where $w(k)$ are Wiener filter coefficients, $\langle ... \rangle$ the expected value, and p the filter's order. Equation (7) can be rewritten in matrix form and efficiently solved using the Levinson recursion algorithm [14]. The filter's optimal order is selected using the model's Bayesian Information Criterion (BIC) [15]. As the system state will evolve and degrade, the prediction error between the modeled reference state and the next state will increase accordingly. Thus the prediction error is chosen as a valuable criterion:

$$\chi_{WF} = \frac{1}{N} \sum_{n=0}^{N-1} \left| x_2(n) - \sum_{k=0}^{p} w(k) x_2(n-k) \right|^2 \qquad (8)$$

where $x_2(n)$ is the temporal signal of the next state of the system.

III. Formulation of the test Signals

In order to compare the performances of the proposed methods, non-stationary synthesis signals are constructed based on the information available in the literature on the bearing generalized roughness fault. In [16], this fault is described as a broadband increase of vibration spectrum with the absence of the bearing characteristic fault frequencies. As the fault increases in severity, the magnitude of the broadband effects increases accordingly [16]. As stated in [16], bearing currents greatly contribute to the production of generalized roughness in the bearings. Among the other causes, the loss of lubricant, contaminated or degraded lubricant are also known to produce a generalized roughness fault [16], [17]. The non-stationarity of this fault may come from the random impact process caused by the wide distribution of surface defects as stated in [18]. Thus, bearing vibrations are stochastically time-dependent, that is non-stationary. The test signals constructed in this section are used to qualify and compare some existing signal processing tools used in the field of bearing health monitoring. Note that the test signals are not exactly models of a bearing generalized roughness fault.

A. *Case 1: Signal with random Transients*

The first case considers a signal composed of transients randomly occurring in time, simulating a possible random impact process between the races and balls of the bearing. Derived from previous work [19]–[21], the transients components are modelled as a series of exponentially decaying sinusoidal vibrations:

$$x_k(t) = \sum_{i=1}^{10} A_t \Theta(t - t_{ik}) e^{B_t (t - t_{ik})} \sin\left(2\pi f_{t,k}(t - t_i)\right) \times f(t) \qquad (9)$$

with $f(t) = 1 + 0.25 \times \sin(w_r t)$ describing the transmission path of mode vibration and A_t, B_t and $f_{t,k}$ being the amplitude, damping ratio and resonant frequency of the ith mode, respectively. The resonant frequencies are randomly chosen in the range: $f_t \in [2kHz, \ldots, 5kHz]$. The amplitudes A_t are increased between two states of the monitoring to simulate the evolution of the fault, while the damping ratio is a fixed parameter. In equation (9), the term $\Theta(t - t_{ik})$ is defined as:

$$\Theta(t - t_i) = \begin{cases} 1 & t - t_{ik} \geq 0 \\ 0 & t - t_{ik} < 0 \end{cases} \quad (10)$$

It is used to insert the transients at the random points of time t_{ik}.

In order to obtain a significant amount of transients this process is repeated k times to form the following signal:

$$x(t) = \sum_k x_k(t) \quad (11)$$

A Gaussian background noise is finally added to the simulated signal $x(t)$ as it is always found in real vibration signals. One portion of the temporal test signal and the spectrum of the entire test signal is shown in Fig. 1.

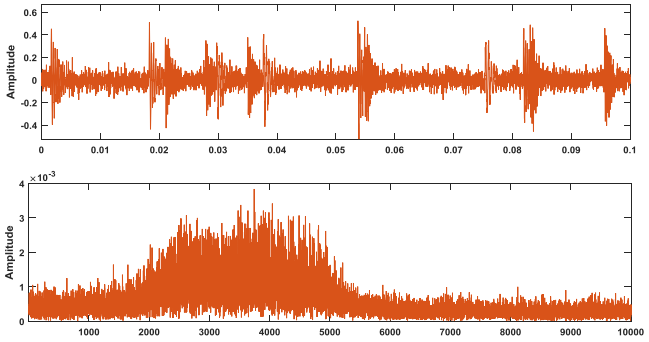

Fig. 1. Test signal with random transients, portion of the temporal signal (top) & spectrum of the entire signal (bottom)

B. Case 2: Non-Stationary Synthesis Vibration Signal

The second case considers a non-stationary vibration signal which is constructed by extrapolation of the sparse information available in the literature concerning the generalized roughness fault.

In accordance with [18], the generalized roughness fault experimentally produced is found to create non-stationary effects in a large frequency band $B_w = [0 - 3333\ Hz]$. Based on [18], a synthesis signal is formulated. It is composed of broadband changes in high-frequency vibrations whose parameters evolve with time in order to simulate the fault severity; thus obtaining a more or less representative image of a developing generalized roughness fault. The reference state signal x_1 with standard deviation σ_1 which could be the signal acquired at the start of a rotating machine during its steady state, is originated from an healthy bearing vibration obtain after maintenance. Its spectral representation is depicted in Fig. 2. It naturally contains periodic components due to shaft rotation, a background noise, resonant frequencies and little amount of non-stationarities. A Gaussian white noise G_{wn} with parameters A_{wn}, μ_{wn} and σ_{wn} is added to x_1 to model the strong background noise. To construct the next state signal, non-stationarities are added in the reference signal within large frequency bands centered around the resonant frequencies of the reference signal. The bands are chosen randomly with constrains and between defined frequency bounds. The non-stationary signal consists in a Gaussian white noise with a zero mean, a time dependent standard deviation $\sigma_{ns}(t)$ linearly increasing along the signal length. It is then filtered around the selected frequency bands. The severity of the bearing degradation can be mimicked by increasing the standard deviation slope $\frac{d\sigma_{ns}}{dt}$. The non-stationary signal is not a bearing fault model but is only used to validate the sensitivities of the proposed methods. Table 1 summarizes the non-stationary signal parameters and Fig. 3 shows an example of a part of the non-stationary signal constrained in the frequency band $[1.36 - 1.73\ kHz]$.

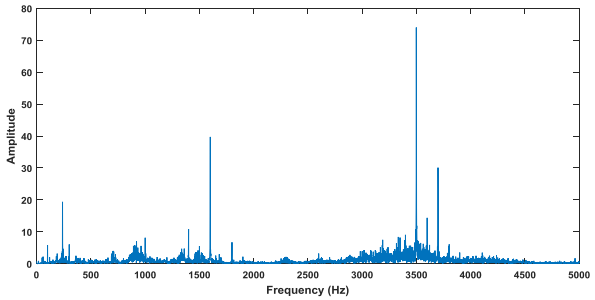

Fig. 2. Healthy bearing spectrum used as the reference state signal

TABLE I. NON-STATIONARY SIGNAL CHARACTERISTICS

Additive background noise	$A_{wn} = \frac{\max(x_1)}{2}$; $\mu_{wn} = 0$; $\sigma_{wn} = \frac{3}{4}\sigma_1$
Fixed frequency bounds (kHz)	$[0.7 - 1.1]$; $[1.2 - 1.8]$; $[2.5 - 4.5]$

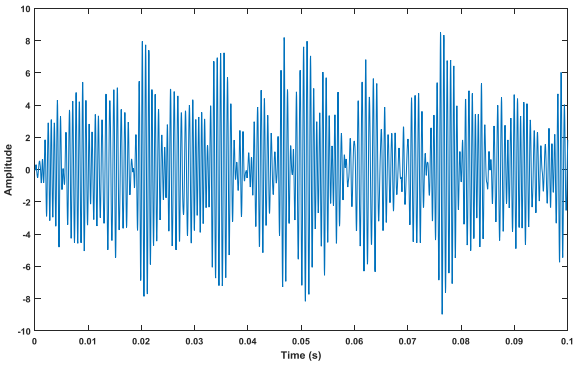

Fig. 3. Part of the non-stationary synthesized signal

IV. SIMULATION RESULTS

A. Signal Processing Methods Comparison

In order to compare the methods, we compute their respective criteria $\chi_{SK}, \chi_{SS}, \chi_{WF}$ on the signal with random transients and on the vibration signal seeded with a broadband non-stationarity from case 1 and case 2 respectively. We defined four different states to emulate the bearing health monitoring: for case 1 the amplitude A_t is linearly increased over time in the range $A_t = 0.2\,..\,1$, while for case 2, the standard deviation slope $\frac{d\sigma_{ns}}{dt}$ is linearly increased over time in the range $\frac{d\sigma_{ns}}{dt} = [0.005\,..\,0.07] \times \kappa_1$, with $\kappa_1 = 0.015\ s^{-1}$.

Concerning the Wiener filtering method: the order is selected for the two different signals corresponding to case 1 and 2 by taking into account the BIC curve with order $p = 1, \ldots, 300$. The BIC criterion is similar to the Akaike Information Criterion (AIC). As the BIC value decreases, the model accuracy increases and a penalty is imposed with the increment of the model order. The optimal order is obtained for the slowest BIC value, or when the BIC decreases slowly [15]. The optimal orders are $p_1 = 22$ and $p_2 = 263$ for reference signal of case 1 and 2 as shown in Fig. 4.

The window length used in spectral kurtosis and spectral subtraction have been optimized to maximize the sensitivities of the criterion defined in section II. All the parameters used for the methods are summarizes in Table 2.

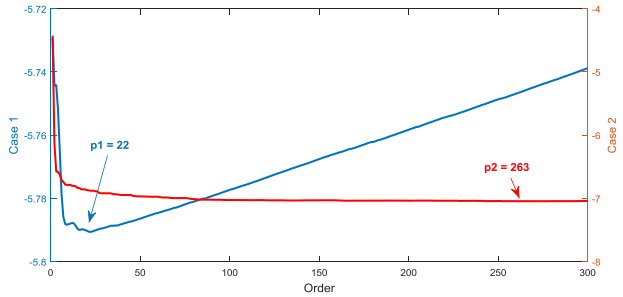

Fig. 4. Wiener Filter order selection via the BIC criteria

TABLE II. DETAILS ON THE METHODS FOR CASE 2

Method – CPU time	Implementation details
Spectral Kurtosis CPU time = 246 ms	Hanning window length = 512 samples Overlap = 75%
Spectral Subtraction CPU time = 398 ms	Hanning window length = 512 samples Overlap = 75%
Wiener filter CPU time = 79 ms	Model order search : find best BIC for $p = 1, \ldots, 300$

Note that the Wiener filtering method consumes less CPU time than the others, which is of importance for implementation an embedded real time application or for a condition monitoring application. The CPU times (Intel® Core™2 3.0GHz) exclude the methods' optimizations which are performed at first iteration. The simulation results are summarized in Table 3. One should be noted that because of the criterion's definition, each first criteria equals zero at the start of the monitoring. The results of case 1 show that all the three methods have good sensitivities for a set of given signal parameters. For the case 2, the simulation pointed out that the SK is no more efficient when the standard deviation slope falls under $\frac{d\sigma_{nsmin}}{dt} = 0.07\ \kappa_1$, contrary to the other two methods whose criterion's order of magnitudes are still consistent. The last two methods have been found to provide a better response to broadband non-stationarities than the SK which seemed more sensitive to signal of case 1. In the hypothesis fixed on the synthetized signals, the results demonstrate that the SK is not always the more effective tool in analyzing certain kind of non-stationarities.

Fig. 5 displays the spectrum of the reference vibration signal (case 2) along with a highly degraded stage with large broadband changes (case 2) with $\frac{d\sigma_{ns}}{dt} = \frac{5}{2}\kappa_1$. It presents strong resemblance with the spectrum obtained in [16], [17] for a bearing generalized roughness fault.

		Case 1	Case 2
	Parameters	$A_{t1} = 0.2$ $A_{t2} = 0.4$ $A_{t3} = 0.7$ $A_{t4} = 1$	$\frac{d\sigma_{ns1}}{dt} = 5 \times 10^{-3} \times \kappa_1$ $\frac{d\sigma_{ns2}}{dt} = 2.5 \times 10^{-2} \times \kappa_1$ $\frac{d\sigma_{ns3}}{dt} = 4.5 \times 10^{-2} \times \kappa_1$ $\frac{d\sigma_{ns4}}{dt} = 7 \times 10^{-2} \times \kappa_1$
Methods	Spectral Kurtosis	$\chi_{SK_1} = 0$ $\chi_{SK_2} = 1.8$ $\chi_{SK_3} = 3.4$ $\chi_{SK_4} = 6.3$	$\chi_{SK_1} = 0$ $\chi_{SK_2} = -2.7 \times 10^{-1}$ $\chi_{SK_3} = -2.6 \times 10^{-1}$ $\chi_{SK_4} = 4.1 \times 10^{-1}$
	Spectral Subtraction	$\chi_{SS_1} = 0$ $\chi_{SS_2} = 5.8 \times 10^{-4}$ $\chi_{SS_3} = 1.4 \times 10^{-3}$ $\chi_{SS_4} = 2.4 \times 10^{-3}$	$\chi_{SS_1} = 0$ $\chi_{SS_2} = 1.5 \times 10^{-4}$ $\chi_{SS_3} = 1.7 \times 10^{-4}$ $\chi_{SS_4} = 1.9 \times 10^{-4}$
	Wiener filter	$\chi_{WF_1} = 0$ $\chi_{WF_2} = 1.9 \times 10^{-3}$ $\chi_{WF_3} = 4.0 \times 10^{-3}$ $\chi_{WF_4} = 6.2 \times 10^{-3}$	$\chi_{WF_1} = 0$ $\chi_{WF_2} = 2.7 \times 10^{-3}$ $\chi_{WF_3} = 3.0 \times 10^{-3}$ $\chi_{WF_4} = 3.5 \times 10^{-3}$

TABLE III. SIMULATION RESULTS FOR THE STUDIED METHODS

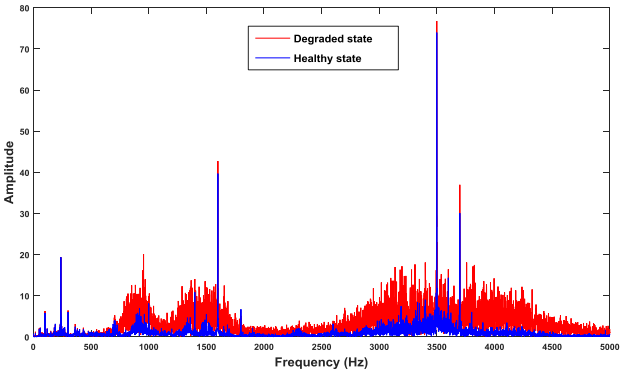

Fig. 5. Comparison between a highly degraded state & healthy bearing state for case 2

V. CONCLUSION

The above results illustrate the effectiveness of the proposed methods to quantify the presence of a non-stationary signal. Simulations on test signals have also shown that the indicator made with SK is dependent on the properties of the non-stationary signal demonstrating that an a priori knowledge of the signal to be detected is often necessary. The bearing generalized roughness seems to produce both effects of random transients (signal of case 1) and broadband changes (signal of case 2). In situations where the random transients are dominating over the broadband changes, the SK would be more suited than the spectral subtraction and the Wiener filtering. However if the broadband changes are dominant in the vibration signal (signal of case 2), the Wiener filtering or the spectral subtraction should be utilized. An experimental validation is therefore necessary to conclude on the preferred method to be used. For this purpose, following the work done in [22], [23] where artificial bearing currents are used to degrade the bearings, future work will consist in the production of a realistic generalized roughness fault to assess the performances of the three studied methods on a real application.

REFERENCES

[1] B. Yazici and G. B. Kliman, "An adaptive statistical time-frequency method for detection of broken bars and bearing faults in motors using stator current," *IEEE Trans. Ind. Appl.*, vol. 35, no. 2, pp. 442–452, Apr. 1999.

[2] V. Climente-Alarcon, J. A. Antonino-Daviu, F. Vedreno-Santos, and R. Puche-Panadero, "Vibration Transient Detection of Broken Rotor Bars by PSH Sidebands," *IEEE Trans. Ind. Appl.*, vol. 49, no. 6, pp. 2576–2582, Nov. 2013.

[3] D.-M. Yang, "Induction Motor Bearing Fault Detection with Non-stationary Signal Analysis," presented at the Mechatronics, ICM2007 4th IEEE International Conference on, 2007, pp. 1–6.

[4] S. Rajagopalan, J. A. Restrepo, J. M. Aller, T. G. Habetler, and R. G. Harley, "Nonstationary Motor Fault Detection Using Recent Quadratic Time–Frequency Representations," *IEEE Trans. Ind. Appl.*, vol. 44, no. 3, pp. 735–744, 2008.

[5] F. Bolaers, O. Cousinard, P. Marconnet, and L. Rasolofondraibe, "Advanced detection of rolling bearing spalling from de-noising vibratory signals," *Control Eng. Pract.*, vol. 12, no. 2, pp. 181–190, Feb. 2004.

[6] Y.-H. Chen, S.-J. Ruan, and T. Qi, "An automotive application of real-time adaptive Wiener filter for non-stationary noise cancellation in a car environment," presented at the Signal Processing, Communication and Computing (ICSPCC), 2012 IEEE International Conference on, 2012, pp. 597–601.

[7] J. Antoni and R. B. Randall, "Unsupervised noise cancellation for vibration signals: part II—a novel frequency-domain algorithm," *Mech. Syst. Signal Process.*, vol. 18, no. 1, pp. 103–117, Jan. 2004.

[8] C. L. Nikias and J. M. Mendel, "Signal processing with higher-order spectra," *IEEE Signal Process. Mag.*, vol. 10, no. 3, pp. 10–37, Jul. 1993.

[9] J. Antoni, "The spectral kurtosis: a useful tool for characterising non-stationary signals," *Mech. Syst. Signal Process.*, vol. 20, no. 2, pp. 282–307, Feb. 2006.

[10] J. Antoni, "Fast computation of the kurtogram for the detection of transient faults," *Mech. Syst. Signal Process.*, vol. 21, no. 1, pp. 108–124, Jan. 2007.

[11] Z. Obeid, A. Picot, S. Poignant, J. Regnier, O. Darnis, and P. Maussion, "Experimental comparison between diagnostic indicators for bearing fault detection in synchronous machine by spectral Kurtosis and energy analysis," presented at the IECON 2012 - 38th Annual Conference on IEEE Industrial Electronics Society, 2012, pp. 3901–3906.

[12] E. H. E. Bouchikhi, V. Choqueuse, and M. E. H. Benbouzid, "Current Frequency Spectral Subtraction and Its Contribution to Induction Machines' Bearings Condition Monitoring," *IEEE Trans. Energy Convers.*, vol. 28, no. 1, pp. 135–144, Mar. 2013.

[13] Wei Zhou, Bin Lu, T. G. Habetler, and R. G. Harley, "Incipient Bearing Fault Detection via Motor Stator Current Noise Cancellation Using Wiener Filter," *IEEE Trans. Ind. Appl.*, vol. 45, no. 4, pp. 1309–1317, Jul. 2009.

[14] M. H. Hayes, *Statistical digital signal processing and modeling*. New York: John Wiley & Sons, 1996.

[15] S. D. Fassois, "IDENTIFICATION, MODEL-BASED METHODS," in *Encyclopedia of Vibration*, Elsevier, 2001, pp. 673–685.

[16] J. R. Stack, T. G. Habetler, and R. G. Harley, "Fault Classification and Fault Signature Production for Rolling Element Bearings in Electric Machines," *IEEE Trans. Ind. Appl.*, vol. 40, no. 3, pp. 735–739, May 2004.

[17] A. A. Elfeky, M. I. Masoud, and I. F. El-Arabawy, "Fault Signature Production for Rolling Element Bearings in Induction Motor," presented at the Compatibility in Power Electronics, 2007. CPE '07, 2007, pp. 1–5.

[18] F. Immovilli, M. Cocconcelli, A. Bellini, and R. Rubini, "Detection of Generalized-Roughness Bearing Fault by Spectral-Kurtosis Energy of Vibration or Current Signals," *IEEE Trans. Ind. Electron.*, vol. 56, no. 11, pp. 4710–4717, Nov. 2009.

[19] R. X. Gao and R. Yan, "Non-stationary signal processing for bearing health monitoring," *Int. J. Manuf. Res.*, vol. 1, no. 1, p. 18, 2006.

[20] Y.-T. Sheen, "On the study of applying Morlet wavelet to the Hilbert transform for the envelope detection of bearing vibrations," *Mech. Syst. Signal Process.*, vol. 23, no. 5, pp. 1518–1527, Jul. 2009.

[21] D. Wang, P. W. Tse, and K. L. Tsui, "An enhanced Kurtogram method for fault diagnosis of rolling element bearings," *Mech. Syst. Signal Process.*, vol. 35, no. 1–2, pp. 176–199, Feb. 2013.

[22] A. Prudhom, J. Antonino-Daviu, H. Razik, and V. Climente-Alarcon, "Time-frequency vibration analysis for the detection of motor damages caused by bearing currents," *Mech. Syst. Signal Process.*, vol. 84, pp. 747–762, Feb. 2017.

[23] T. Zika, I. C. Gebeshuber, F. Buschbeck, G. Preisinger, and M. Gröschl, "Surface analysis on rolling bearings after exposure to defined electric stress," *Proc. Inst. Mech. Eng. Part J J. Eng. Tribol.*, vol. 223, no. 5, pp. 787–797, May 2009.